A New Endoluminal, Flow-Disrupting Device for Treatment of Saccular Aneurysms

David F. Kallmes, MD; Yong Hong Ding, MD; Daying Dai, MD; Ramanathan Kadirvel, PhD; Debra A. Lewis, PhD; Harry J. Cloft, MD, PhD

Background and Purpose—We report a preclinical study of a new endoluminal device for aneurysm occlusion to test the hypothesis that the device, even without use of intrasaccular coil placement, could occlude saccular aneurysms without causing substantial parent artery compromise or compromise of adjacent, small branch arteries.

Methods—The Pipeline Neuroendovascular Device (Pipeline NED; Chestnut Medical Technologies, Inc) is a braided, tubular, bimetallic endoluminal implant aimed at occlusion of saccular aneurysms through flow disruption along the aneurysm neck. The device was implanted across the necks of 17 elastase-induced aneurysms in the New Zealand white rabbit model and followed for 1 month (n=6), 3 months (n=5), and 6 months (n=6). In each subject, a second device was implanted in the abdominal aorta to cover the origins of lumbar arteries. Aneurysm occlusion rates by angiography (grade 1, complete occlusion; grade 2, near-complete occlusion; and grade 3, incomplete occlusion) were documented. Percent area stenosis of the parent arteries was calculated. Presence of distal emboli in the downstream vessels in the parent artery and branch artery stenosis or occlusion was noted.

Results—Grades 1, 2, and 3 occlusion rates were noted in 9 (53%), 6 (35%), and 2 (12%) of 17 aneurysms, respectively, indicating an 88% rate of complete or near complete occlusion. No cases of branch artery occlusion or distal emboli in the downstream vessels of the parent artery, specifically the subclavian artery, were seen. Parent artery compromise from neointimal hyperplasia was minimal in most cases.

Conclusions—The Pipeline NED is a trackable, bio- and hemocompatible device able to occlude saccular aneurysms with preservation of the parent artery and small, adjacent branch vessels. **(*Stroke*. 2007;38:2346-2352.)**

Key Words: rabbit ■ saccular aneurysm ■ stent

Although intravascular coil embolization for aneurysms is widely applied, standalone devices aimed at endoluminal reconstruction for treatment of intracranial aneurysms have yet to be developed. Such an endoluminal device may offer substantial advances over endosaccular therapies, including the avoidance of aneurysm perforation and the ability to treat wide-necked aneurysms. Tortuous, distal access needed for intracranial use limits applicability of covered stents used in extracranial applications.[1] Other endoluminal devices such as the Neuroform (Boston Scientific Inc) are able to access distal vasculature but function as adjuncts to coils rather than devices aimed at primary aneurysm occlusion.[2,3]

We describe the in vivo performance of a new endoluminal device aimed at aneurysm occlusion through flow disruption at the aneurysm neck. The Pipeline Neuroendovascular Device (Pipeline NED; Chestnut Medical Technologies, Inc) is a highly trackable, tubular device constructed from platinum and stainless steel that, once deployed in the parent artery, offers approximately 30% coverage of the aneurysm neck by its metallic struts. This high density of coverage is designed to alter flow and, even without intrasaccular coils, induce aneurysm occlusion.

In this study, we report aneurysm occlusion rates, degree and extent of neointimal hyperplasia, and patency rates of small, branch arteries covered by the Pipeline NED using the rabbit elastase aneurysm model.

Materials and Methods

The Pipeline NED is comprised of 16 strands of platinum and 16 strands of stainless steel ribbons. These strands are braided and heat-treated in the expanded configuration. On release from the delivery system and when properly positioned at the desired location in the vessel, the implant expands to cover the neck of the aneurysm (Figure 1A through 1C). The device forms a high-coverage mesh of approximately 30% by area. The Pipeline NED is attached to a flexible delivery wire, which has radiopaque end markers, and packaged in an introducer sheath. This packaged device can be loaded into standard microcatheters of 0.027-inch inner diameter or greater. The device is pushed through the microcatheter and deployed by a combination of microcatheter withdrawal and forward pressure on the delivery wire. The device undergoes approximately 50% shortening during deployment, depending on diameter of the device and parent artery.

Received December 8, 2006; final revision received January 26, 2007; accepted February 20, 2007.

From the Department of Radiology, Mayo Clinic, Rochester, MN.

Correspondence to David F. Kallmes, MD, Department of Radiology, Mayo Clinic, 200 First Street SW, Rochester, MN 55905. E-mail Kallmes.david@mayo.edu

Stroke **is available at http://www.strokeaha.org** **DOI: 10.1161/STROKEAHA.106.479576**

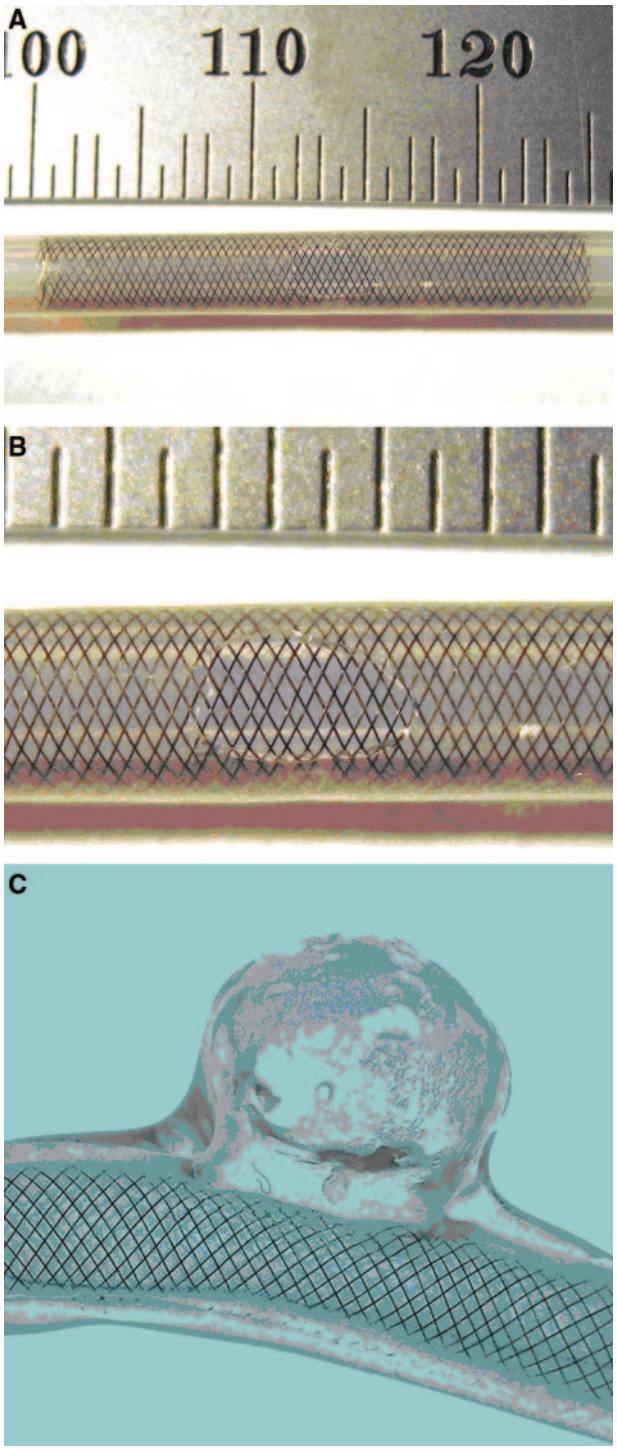

Figure 1. Photographs of the Pipeline Neuroendovascular Device (Pipeline NED). A, Photograph of the Pipeline NED deployed in a 3.5-mm diameter plastic model. B, Higher magnification of the model at the site of the orifice of a model aneurysm showing the coverage of the orifice by the device struts. C, Lateral view of the Pipeline NED deployed across the neck of a model aneurysm.

In Vivo Experiments

Aneurysms (n=17) were created in New Zealand white rabbits as previously described.[4] Aneurysms were allowed to mature for at least 21 days before embolization.[5] Two days before embolization, subjects were premedicated with aspirin (10 mg/kg orally) and clopidogrel (10 mg/kg orally). Anesthesia was induced using 74 mg/kg ketamine, 5 mg/kg xylazine, and 1 mg/kg acepromazine and maintained using ketamine (10 mg/kg) and xylazine (3 mg/kg). A surgical cutdown of the right femoral artery was performed and a 5-Fr sheath inserted. A 5-Fr guide catheter (Envoy; Cordis) was placed into the aortic arch and digital subtraction angiography (DSA) performed. Heparin (500 U intravenously) was administered and then a microcatheter (Renegade HiFlow; Boston Scientific) was placed over a microguidewire (Transcend; Boston Scientific) into the subclavian artery distal to the aneurysm cavity. The wire was removed and the Pipeline NED was advanced into the distal aspect of the microcatheter. The device was deployed across the neck of the aneurysm and, in most cases, across the neck of the right vertebral artery. The microcatheter was removed and DSA performed of the aortic arch. The guiding catheter was retracted and placed in the abdominal aorta and DSA performed. An additional Pipeline NED was placed in the aorta across the origin of at least one pair of lumbar arteries and DSA performed. The guiding catheter and sheath were removed. The femoral artery was ligated. Animals were allowed to recover. Antiplatelet therapy was continued for 30 days after embolization. Subjects were followed for 1 month (n=6), 3 months (n=5), and 6 months (n=6). At the time of killing, animals were deeply anesthetized. DSA of the aortic arch and the abdominal aorta was performed. Animals were then killed with a lethal injection of pentobarbital. Harvested aneurysms and aorta were immediately fixed in 10% neutral buffered formalin. A single aneurysm, from the 3-month group, was processed for scanning electron microscopy.

Data Analysis

Angiographic Evaluation

The follow-up angiography assessed aneurysm occlusion using a 3-point scale, including grade 1, complete occlusion; grade 2, near occlusion; and grade 3, incomplete occlusion. Patency of the branch arteries, including lumbar and vertebral arteries covered by the devices, was assessed.

Conventional Histopathologic Processing and Analysis

The diameters of the lumbar vertebral arteries covered by the devices were measured under the dissection microscope at the ostia. After routine tissue processing, the fixed samples were embedded in paraffin. Samples were then cut axially at 1000 μm using an Isomet low-speed saw (Buehler). The metal stents were carefully removed under a dissecting microscope. The samples were then reembedded in paraffin, sectioned at 5 to 6 μm, and stained with hematoxylin and eosin (H&E). Two experienced observers evaluated the histologic sections. Axial sections were taken from the proximal, mid-, and distal portions of the aortic stented segment and from the proximal and distal portions of the aneurysm's parent artery. Morphometric measurements were performed using digital planimetry with a calibrated microscope system. The system included a Sport RT Digital Camera (Diagnostic Instruments) attached to an Olympus BH2 microscope. Measurements were obtained using Sport RT software version 3.0 (Diagnostic Instruments). The external elastic lamina area, internal elastic lamina area and luminal area were measured. Neointimal thickness was measured as the distance from the inner surface of each stent strut to the luminal border. A vessel injury score was calculated according to the Schwartz method.[6] Calculations made from the morphometric measurements were as follows: neointimal area=internal elastic lamina area−luminal area;

TABLE 1. Summary of Aneurysm Sizes by Group

Time, month(s)	Neck, mm	Width, mm	Height, mm
1	2.9±1.5	3.6±0.8	8.0±2.3
3	2.7±1.2	3.8±0.7	7.7±2.1
6	3.2±0.7	3.8±0.9	8.0±2.1

Data are represented as mean±SD. There were no significant differences between time points.

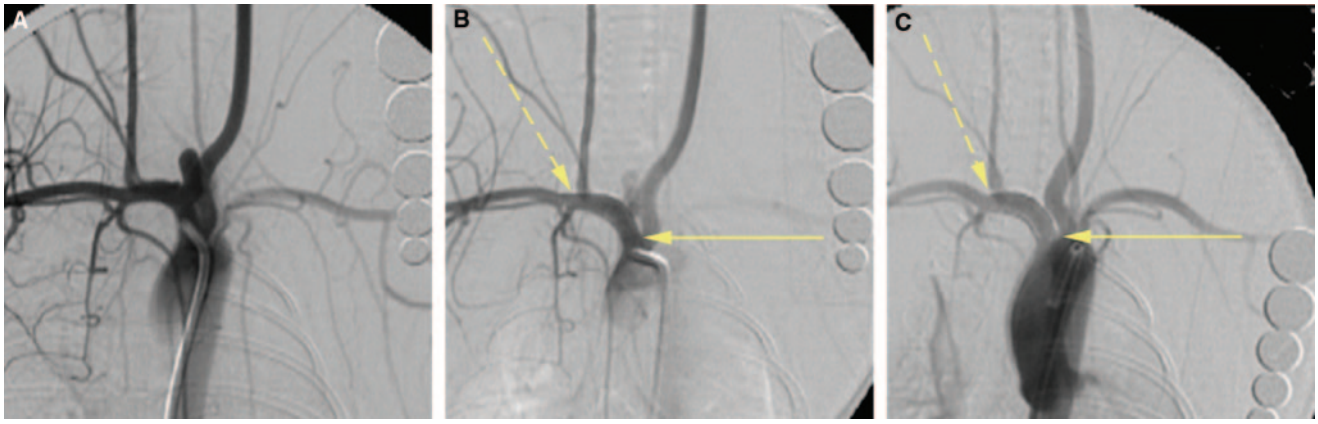

Figure 2. Representative angiograms from the 1-month group. A, DSA before stent implantation showing the aneurysm. B, DSA image immediately postimplantation showing partial occlusion of the aneurysm. The right vertebral artery is patent. C, DSA image when the animal was killed showing the aneurysm is completely occluded. The right vertebral artery remains patent. The yellow arrow indicates the proximal end of the stent and the dashed yellow arrow indicates distal end of the stent.

percent stenosis=(injured luminal area÷internal elastic lamina area)×100; mean injury score=[(sum of injury scores for each strut)÷number of struts; mean neointimal thickness=[(sum of neointimal thickness)÷number of struts.

Tissue Processing for Scanning Electron Microscopy

After follow-up angiography, the stented arteries from one of five subjects at the 3-month time point were harvested for scanning electron microscopy. The subject was deeply anesthetized and then pressure-perfused with 0.9% saline followed by a fixative solution of 4.0% paraformaldehyde with 2.5% glutaraldehyde at systemic pressure. The stented arteries were then harvested and fixed in scanning electron microscopy fixative solution 4.0% paraformaldehyde with 2.5% glutaraldehyde in 0.1 mol/L phosphate buffer, pH 7.4. After fixation, the stented arteries were gently opened to expose the aneurysm neck and the ostium of the lumbar artery. Then the samples were rinsed 3 times in phosphate buffer at 24°C. They were postfixed for 1 hour in 1.0% osmium tetroxide in distilled water, washed three times in phosphate buffer, and dehydrated in graded ethanols. The stented arteries were then dried in a Tousimis Samdri-780 critical-point dryer using liquid carbon dioxide as the transitional fluid. After critical point drying, the samples were affixed to specimen mounts with Avery "Spot-o-Glue" and coated with approximately 20 nm of a gold/palladium alloy in a Technics Hummer V sputter coater (MRTL). Finally, we examined the occlusion of the aneurysm neck and the patency of lumbar arteries and the right vertebral artery with a JEOL 6400 scanning electron microscopy (JEOL, Ltd).

Statistical Analysis

Measurements were made at the proximal, middle, and distal ends of the abdominal aorta stent. The stent embolizing the aneurysm was divided into 2 parts; from the distal edge of the neck to the distal end of the stent was termed the distal stent and the proximal edge of the neck to the proximal end of the stent was termed the proximal stent. Each distal and proximal stent was then divided, depending on size, into 2 (proximal and distal) segments or 3 segments (proximal, middle, and distal). These segments were averaged together to obtain one representative number for the stent for each variable. The only exception to this was percent stenosis. In this case, we used the highest calculated value as the representative value for the stent. Values for injury score, neointimal thickness, and percent stenosis were compared between stent locations (proximal and distal) for each aneurysm over the different time points using a 2-way analysis of variance (time*location; JMP; SAS Inc.; $P<0.05$); values for stents placed in the abdominal aorta were compared over time using a one-way analysis of variance (JMP; SAS Inc.; $P<0.05$). If significant differences were found with these tests, then a Student t test was used to make post hoc comparisons ($P<0.05$).

Results

Aneurysm sizes are shown in Table 1. Fusiform dilation of the parent artery distal to the aneurysm cavity was present in 7 (44%) of 17 cases. Overall, grade 1, 2, and 3 occlusion rates were noted in 9 (53%), 6 (35%), and 2 (12%) of 17 aneurysms

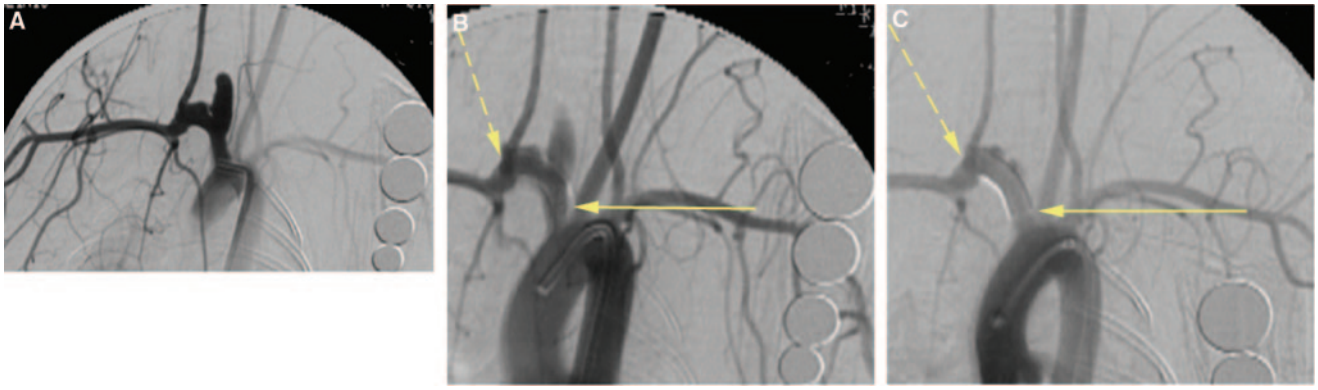

Figure 3. Representative angiograms from the 3-month group. A, DSA before stent implantation shows the aneurysm. B, DSA image immediately postimplantation showing that part of the aneurysm dome is occluded. The right vertebral artery is patent. C, DSA image after the animal was killed; most of the aneurysm lumen is occluded with a small neck remnant and fusiform dilation remaining patent. The right vertebral artery is patent. The yellow arrow indicates the proximal end of the stent and the dashed yellow arrow indicates distal end of the stent.

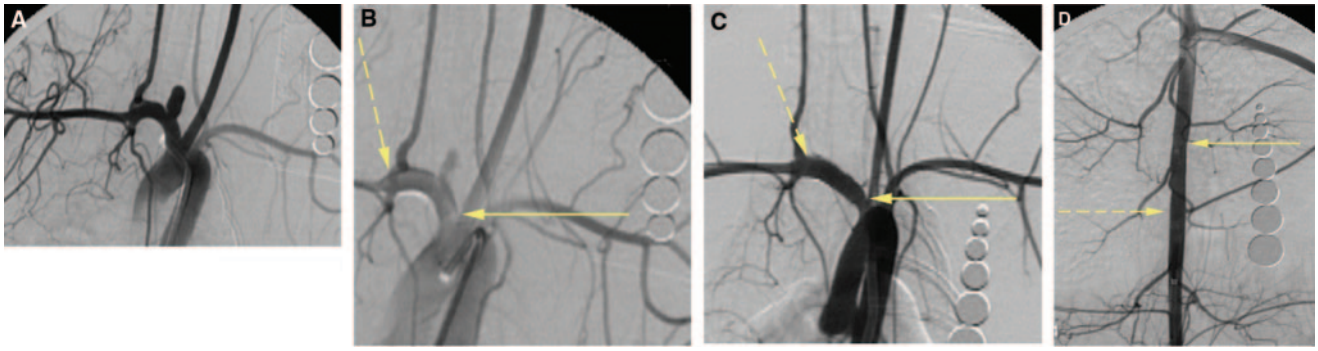

Figure 4. Representative angiograms from the 6-month group. A, DSA before stent implantation showing the aneurysm. B, DSA image immediately postimplantation; part of the aneurysm cavity is occluded, whereas the right vertebral artery remains patent. C, DSA image when the animal was killed showing that the aneurysm is completely occluded. The right vertebral artery remains patent. D, DSA image of the abdominal aorta when the animal was killed showing the lumbar arteries covered by the device remaining patent. The yellow arrow indicates the proximal end of the stent and the dashed yellow arrow indicates the distal end of the stent.

(not significant, $P=0.0993$), respectively (Figures 2, 3, and 4). At 1 month, grade 1, 2, and 3 occlusion rates were noted in 3, 2, and one case, respectively. At 3 months, grade 1 and 2 occlusion rates were noted in 2 and 3 cases, respectively. At 6 months, grade 1, 2, and 3 occlusion rates were noted in 4, one, and one case, respectively.

Mean diameter of the lumbar artery origin was 1.3±0.4 mm. Mean diameter of the vertebral artery origin was 1.4±0.6 mm. No cases of branch artery occlusion or distal emboli were seen. All branch arteries covered by the devices remained patent at follow up. Fusiform dilation covered by the device remained patent in 6 of 7 cases (Figure 3). Parent artery compromise from neointimal hyperplasia was minimal except in distal arteries harboring oversized devices and diminished after 3 months (Tables 2 and 3). Morphometric measurements of the histologic findings are shown in Tables 2 and 3.

Conventional histopathology showed that at 1 month, the aneurysm domes were primarily filled with unorganized thrombus. Neointima, along with the struts across the neck, was noted in 3 of 6 aneurysms (Figure 5A). Moderately thick intimal hyperplasia was noted at the distal stent portion of the parent artery in 3 of 6 aneurysms and was mild in the remaining 3 subjects. Intimal hyperplasia in the stented aorta was minimal in all 6 subjects.

At 3 months, one of 4 aneurysms had organized connective tissue occupying the dome, whereas the other 3 aneurysms had poorly organized thrombus, which partially filled the dome. Neointima that partially covered the neck was observed in 2 of 4 subjects. The local tissue appeared to have features resembling cartilaginous tissue accompanied by calcification in the parent arteries of all 4 subjects. Cartilaginous tissue associated with calcification was also observed at the stented aortic wall in one subject. Intimal hyperplasia in the stented aorta was similar to that seen at 1 month.

TABLE 2. Morphometric Measurements in Aortic Segments

Time, month(s)	Injury Score	Neointimal Thickness, mm	Stenosis, %
1	0.0±0.0	0.2±0.1	20±5
3	0.3±0.2	0.2±0.1	16±5
6	0.1±0.2	0.1±0.0	15±6

Data are represented as mean±SD. There were no significant differences among time points.

Six months after implantation, 4 of 6 aneurysms had a thick neointima along with stent struts covering the neck (Figure 5B). Two of 6 aneurysms had organized tissue filling the dome; the other 4 had poorly organized thrombus partially occupying the dome. The intima hyperplasia along the distal parent artery beyond the aneurysm (Figure 5C) and in the stented aorta remained slight (Figure 5D) in all 6 subjects. Calcification and/or ossification were noted in the stented parent artery and aorta in all 6 subjects (Figure 6A and 6B). The vertebral and lumbar artery ostia, which had the stents overlying them, were all patent in all subjects at all 3 time points (Figure 6C and 6D). There was no evidence of an inflammatory response to the stents at any time point.

The percent stenosis in the distal stent of parent artery at 6 months was significantly lower than that at 1 month (Tables 2 and 3). There were no significant differences in the injury scores or neointimal thickness. There were no significant differences in the injury scores, neointimal thickness, or percent stenosis in the stented aorta.

Scanning electron microscopy performed for one subject, 3 months after implantation, demonstrated that the aneurysm was completely occluded. The ostia under the stented portions of the lumbar and right vertebral arteries were all patent (Figure 6E). The endothelial cells, which covered the stent, were contiguous to the endothelium of the parent artery or aorta.

Discussion

In this study, we report efficacy and safety data from a new endoluminal device aimed at occlusion of saccular aneurysms. The device was highly trackable and of appropriate radiopacity for endovascular placement using standard radiographic equipment. Using the Pipeline NED, we achieved an 88% rate of complete or near complete aneurysm occlusion with only minimal degrees of neointimal hyperplasia that diminished substantially over time. This rate of complete or near complete aneurysm occlusion is relatively similar to previous work in the model using a variety of coil devices.[7] Furthermore, small branch arteries remained patent even

TABLE 3. Morphometric Measurements in Aneurysm-Bearing Arterial Segments

Time, month(s)	Injury Score		Neointimal Thickness, mm		Stenosis, %	
	Proximal*	Distal†	Proximal	Distal	Proximal	Distal
1	0.0±0.0	0.1±0.2	0.2±0.0	0.2±0.0	22±2‡	38±13
3	0.1±0.1	0.2±0.2	0.2±0.1	0.1±0.1	35±18	30±10
6	0.0±0.0	0.1±0.1	0.2±0.1	0.1±0.0	23±8	17±8§

Data are represented as mean±SD.
*Proximal indicates the proximal end of the stented parent artery.
†Distal indicates distal end of stented parent artery.
‡A significant difference in percent stenosis between proximal and distal locations at 1 month ($P<0.05$).
§A significant difference in percent stenosis between distal segments at 1 and 6 months ($P<0.05$).

when covered by the device. These data offer promise that the Pipeline NED will permit excellent rates of aneurysm occlusion while preserving patency of the parent artery and adjacent branch vessels.

Other endoluminal devices have been proposed for use in treating intracranial aneurysms. The JoStent (Abbott Vascular) is a covered stent that was used to treat a cohort of 25 patients harboring proximal intracranial aneurysms with excellent results.[1] The mechanism of action in the JoStent is different from that of the Pipeline NED, because the covering of the JoStent directly occludes the aneurysm cavity. However, the JoStent is stiff compared with most neuroendovascular devices and may be difficult or impossible to place within the intracranial vasculature. The Neuroform represents an endoluminal device that is designed as an adjunct to coil embolization and not to induce primary closure of the aneurysm cavity. One series reported the ability of the Neuroform device to occlude small aneurysms without coils, but the ability of the Neuroform to treat other types of aneurysms without adjunctive coils is unknown.[8]

Coverage of adjacent parent arteries such as the ophthalmic artery, the posterior communicating artery, and the anterior choroidal artery by an endoluminal device may lead to concerns regarding untoward occlusion of these vessels. The rabbit descending aorta has previously been used as a model for stents intended for intracranial use, especially regarding their impact on small, branch vessels.[9] In our model, we noted excellent patency of small, branch arteries covered by the device. We hypothesize that continued flow in these arteries permits ongoing patency, whereas aneurysm cavities, which lack an outflow channel, undergo thrombosis. With rapid flow in an artery across the device struts, there is no tendency for occlusion. However, when placed across the aneurysm neck, the device slows the flow and allows occlusion. Our model is imperfect for predicting patency of branch or perforating arteries in humans, because we studied arteries on the order of 1.3 to 1.5 mm in diameter but at least offer hope that branch arteries covered by the device will remain patent.

Degree of neointimal hyperplasia varied in this study depending on where the hyperplasia was measured. The rabbit brachiocephalic/subclavian artery tapers along its course, but we chose to size the device based on the most proximal aspect of the vessel. For this reason, devices were relatively oversized in the distal aspect of the parent artery but

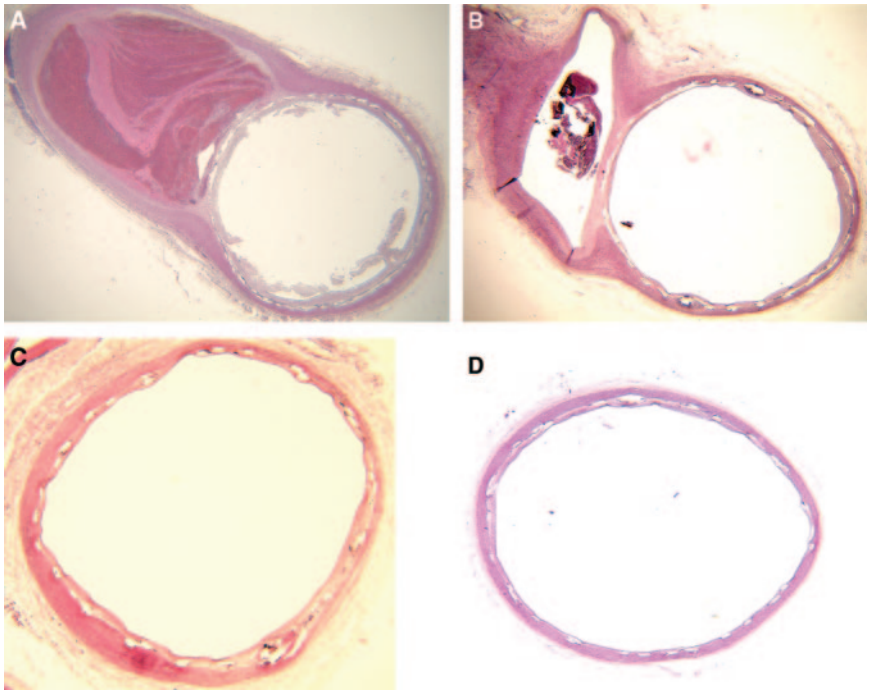

Figure 5. Photomicrographs of the embolized aneurysms at (A) 1 and (B–D) 6 months after implantation. A, The neointima along the stent struts; the neointima runs completely across the aneurysm neck. There is poorly organized thrombus throughout the dome and intimal hyperplasia is mild in the parent artery (H&E, original magnification ×20). B, A thick neointima along the stent struts at 6 months, which completely covers the aneurysm neck. Unorganized thrombus within the dome was also noted and intimal hyperplasia in the parent artery was minimal (H&E, original magnification ×20). C, The distal end of the distal portion of the parent artery; intimal hyperplasia was mild (H&E, original magnification ×40). D, A photomicrograph of the stented aorta showing slight neointimal hyperplasia (H&E, original magnification ×25).

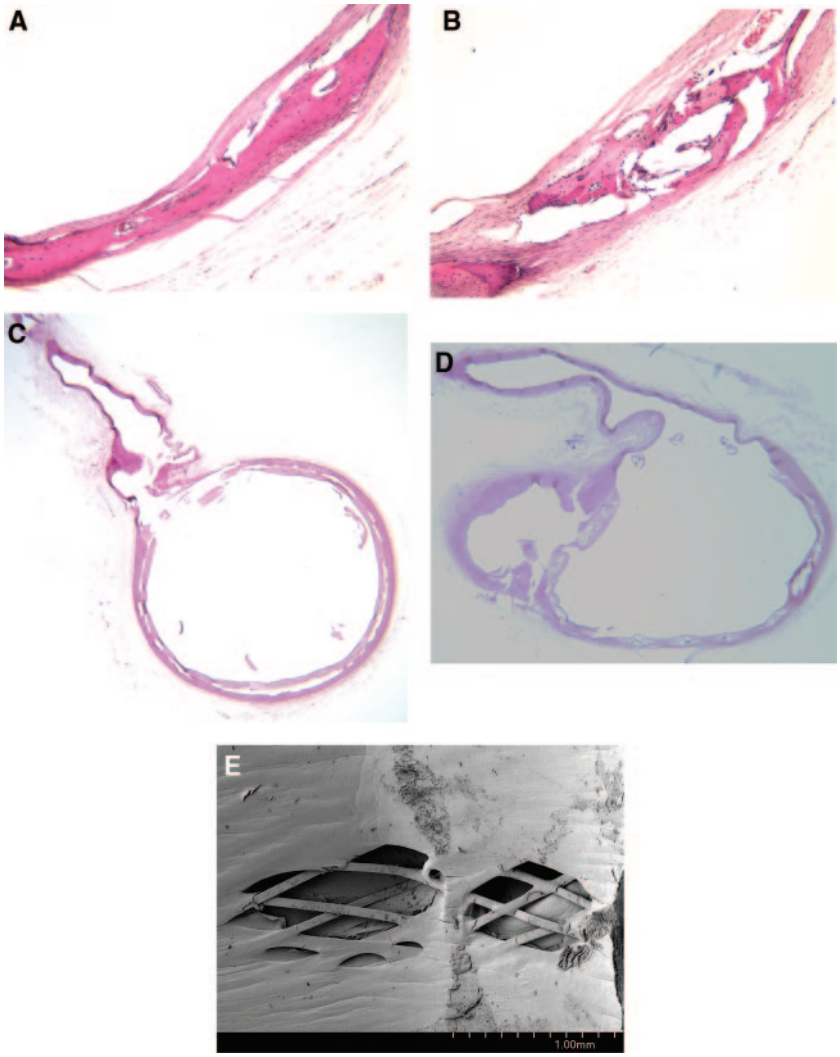

Figure 6. Photomicrographs 6 months after implantation (A–D) and scanning electron photograph 3 months after implantation (E). A, The photomicrograph taken from the distal parent artery showing the bone-like tissue (H&E, original magnification ×150). B, A photomicrograph taken from the stented aorta showing the bone-like tissue at the wall (H&E, original magnification ×150). C, A photomicrograph of the stented aorta showing the ostium of the lumbar artery is patent 6 months after implantation (H&E, original magnification ×15). D, A photomicrograph of the distal parent artery showing the ostium of the vertebral artery is patent 6 months after implantation (H&E, original magnification ×30). E, The scanning electron photograph 3 months after stenting; it shows the ostia of lumbar arteries are patent. The stent struts crossing the ostia are partially covered with regenerated endothelial-like cells, which are in contact with the aorta (scanning electron microscopy, original magnification ×50).

were appropriately sized in the proximal aspect of the brachiocephalic artery and throughout the aortic devices. When properly sized, percent area stenosis was on the order of a maximum of 15%. Furthermore, percent area stenosis diminished over time in the areas most affected at earlier time points.

We report injury score in this study, although injury scores historically have been confined to studies of stents aimed at coronary artery applications. In brief, injury scores of less than 0.4 indicate minimal injury, which was found consistently in this study.[10]

It remains possible that the Pipeline NED may offer particular challenges for subsequent aneurysm treatment if the treatment with the Pipeline NED fails to achieve complete occlusion. Traversing the device with a microcatheter for coil placement in cases of incomplete closure will be difficult given the small interstrut dimensions of the device. Thus, additional treatment in such cases may be limited to placement of a second device to achieve further closure.

The devices tested in this project were first generation. Since completion of this project, substantial improvements in design have been achieved. Ongoing experiments are testing the efficacy and safety profiles of newer generation Pipeline NED designs.

We noted cartilaginous and bone-like transformation of tissues around some devices at later time points. We and others have noted such transformation in experimental aneurysms treated with coils.[11,12] A recent review of the mechanism of calcification within atherosclerotic plaque noted that both the cellular and soluble factors required for bone formation are present in plaque.[13] The exact relevance of the findings in the current study is unknown.

This study has numerous limitations. We did not include a control group of untreated aneurysms or aneurysms treated by other means. However, historical data has shown near perfect rates of long-term patency of elastase-induced aneurysms, up to 2 years.[14] These historical controls probably are appropriate for comparison to the current work. Furthermore, this work describes outcomes using a first-generation device, and we anticipate that further refinement of the device will improve occlusion rates. In addition, the neck diameter and aneurysm size is relatively small compared with many of the broad-necked aneurysms that likely will be treated in humans, so occlusion rates in this model may overestimate those that will be seen in humans. Last, the trackability of the device is difficult to assess in any preclinical model, because tortuosity of the model does not mimic that of the carotid siphon.

However, in benchtop test models, the Pipeline NED system traverses with ease through a torturous path that is similar to the neurovasculature (unpublished data). The Pipeline NED has also been tested in canine and swine models, and it was shown to reach distal vessels without difficulty (unpublished data).

Source of Funding

This study was funded by Chestnut Medical Technologies, Inc, Menlo Park, CA.

Disclosures

None.

References

1. Saatci I, Cekirge HS, Ozturk MH, Arat A, Ergungor F, Sekerci Z, Senveli E, Er U, Turkoglu S, Ozcan OE, Ozgen T. Treatment of internal carotid artery aneurysms with a covered stent: experience in 24 patients with mid-term follow-up results. *AJNR Am J Neuroradiol*. 2004;25: 1742–1749.
2. Fiorella D, Albuquerque FC, Deshmukh VR, McDougall CG. Usefulness of the Neuroform stent for the treatment of cerebral aneurysms: results at initial (3–6-mo) follow-up. *Neurosurgery*. 2005;56:1191–1201; discussion 1201–1192.
3. Lylyk P, Ferrario A, Pasbon B, Miranda C, Doroszuk G. Buenos Aires experience with the Neuroform self-expanding stent for the treatment of intracranial aneurysms. *J Neurosurg*. 2005;102:235–241.
4. Altes TA, Cloft HJ, Short JG, DeGast A, Do HM, Helm GA, Kallmes DF. 1999 ARRS Executive Council Award. Creation of saccular aneurysms in the rabbit: a model suitable for testing endovascular devices. American Roentgen Ray Society. *AJR Am J Roentgenol*. 2000;174:349–354.
5. Fujiwara NH, Cloft HJ, Marx WF, Short JG, Jensen ME, Kallmes DF. Serial angiography in an elastase-induced aneurysm model in rabbits: evidence for progressive aneurysm enlargement after creation. *AJNR Am J Neuroradiol*. 2001;22:698–703.
6. Schwartz RS, Huber KC, Murphy JG, Edwards WD, Camrud AR, Vlietstra RE, Holmes DR. Restenosis and the proportional neointimal response to coronary artery injury: results in a porcine model. *J Am Coll Cardiol*. 1992;19:267–274.
7. Ding YH, Dai D, Lewis DA, Cloft HJ, Kallmes DF. Angiographic and histologic analysis of experimental aneurysms embolized with platinum coils, Matrix, and Hydrocoil. *AJNR Am J Neuroradiol*. 2005;26: 1757–1763.
8. Fiorella D, Albuquerque FC, Deshmukh VR, Woo HH, Rasmussen PA, Masaryk TJ, McDougall CG. Endovascular reconstruction with the Neuroform stent as monotherapy for the treatment of uncoilable intradural pseudoaneurysms. *Neurosurgery*. 2006;59:291–300; discussion 291–300.
9. Masuo O, Terada T, Walker G, Tsuura M, Matsumoto H, Tohya K, Kimura M, Nakai K, Itakura T. Study of the patency of small arterial branches after stent placement with an experimental in vivo model. *AJNR Am J Neuroradiol*. 2002;23:706–710.
10. Virmani R, Farb A. Assessing the advantages and disadvantages of novel radiation therapy for vascular restenosis: injury score, artery size, and short lengths. *Cardiovasc Radiat Med*. 1999;1:308–310.
11. Dai DM, Ding YH, Kadirvel R, Lewis DA, Cloft HJ, Kallmes DF. Bone formation in elastase-induced rabbit aneurysms embolized with platinum coils: report of two cases. *AJNR Am J Neuroradiol*. 2007;28:1176–1178.
12. Killer M, Richling B, Minnich B, Lametschwandtner A, Plenk H. Unexpected tissue engineering: cartilage neoformation in long-term Hydrocoil ®-occluded experimental aneurysms. *European Cells and Materials*. 2004; 7(suppl 1):43.
13. Doherty TM, Fitzpatrick LA, Inoue D, Qiao JH, Fishbein MC, Detrano RC, Shah PK, Rajavashisth TB. Molecular, endocrine, and genetic mechanisms of arterial calcification. *Endocr Rev*. 2004;25:629–672.
14. Ding YH, Dai D, Lewis DA, Danielson MA, Kadirvel R, Cloft HJ, Kallmes DF. Long-term patency of elastase-induced aneurysm model in rabbits. *AJNR Am J Neuroradiol*. 2006;27:139–141.